AN APPROACH TO SOLVING COUPLED EQUATIONS THAT MAY ARISE FROM APPLICATIONS OF LAPLACE'S EQUATION*

by

D. D. Hearn, M. Summers and G. Wilson
Western Illinois University

ABSTRACT

Illustrating a general approach that may be used to obtain the electrostatic field between conducting objects, a solution of Laplace's equation is presented for the case of a conducting, right circular cylinder between parallel, charged conducting plates. The analytical expressions derived from this boundary value problem for the electric potential function and the corresponding electric field intensity are in the form of coupled, nonlinear equations. These equations are solved numerically by iteration for a designated parameter set, specifying one possible geometry and position of the cylinder.

---

* This research was supported in part by the Defense Nuclear Agency under Contract L37AAXYX970.

INTRODUCTION

Objects susceptible to electromagnetic interference are often tested for the effects of such interference by guiding a pulse of electromagnetic energy over the objects and experimentally determining their response to this field. In such cases, it is desirable to know the electric field values at various points over the object for the principal or TEM (transverse electromagnetic) mode of propagation. These field values may be estimated from the known field distribution about the transmission line when no test object is present [1]. However, more accurate values are often required, and it is the purpose of this paper to provide analytical expressions for the field distribution about a cylindrical test object and to discuss a numerical approach to solving these expressions. This example also illustrates a general approach that may be applied to similar boundary value problems.

For the TEM propagation mode, the field distribution of the propagating pulse can be obtained from electrostatic theory. Thus the problem is one of solving a suitable form of Laplace's equation with appropriate boundary conditions. Boundary conditions for this problem are determined from the following physical arrangement. A conducting, right circular cylinder is placed between the conducting surfaces of a transmission line with the cylindrical axis perpendicular to the conducting surfaces, as diagrammed in Figure 1. The direction of travel of the electromagnetic field is perpendicular to the diagram, and the vertical positioning of the cylinder is arbitrary. Since the cylinder axis is to be located symmetrically with respect to the width w of the transmission line and the radius a is assumed to be small relative to w, field fringing effects can be ignored in this problem. Therefore, the conducting

surfaces bounding the transmission line will be treated as infinite, parallel, conducting plates. Equal and opposite charges will be carried by the plates, while the cylinder is assumed uncharged. These requirements fix the boundary conditions on the electric potential function such that the potential must vanish over the surface of the cylinder, take on equal but oppositely signed values over the two plates, and approach a uniform field potential in the z-direction far from the axis of the cylinder.

A cylindrical coordinate formulation of Laplace's equation is obviously most convenient, since the problem geometry displays cylindrical symmetry. The complicated boundary conditions, however, make it difficult to directly obtain a single equation for the potential function that is valid throughout the entire region between the plates. Consequently, Laplace's equation is solved separately in each of the three overlapping areas. This results in a set of coupled, nonlinear equations for the potential function and electric field intensity which require a numerical, iterative technique for solution.

The derivation of the coupled field equations is described in the following section. A numerical evaluation of these equations is then discussed for specific cylinder dimensions and vertical positioning in the field.

2. SOLUTION OF LAPLACE'S EQUATION

Distribution of the static electric field surrounding a conducting, right circular cylinder between infinite, charged, parallel, conducting plates may be obtained from solutions of Laplace's equation,

$$\nabla^2\Phi = 0, \tag{1}$$

for the physical configuration illustrated in Figure 2. The geometry of the problem clearly implies a solution in terms of cylindrical coordinates. Furthermore, since the plates are taken to be of infinite extent, the potential Φ is independent of the angular cylindrical coordinate. Thus, (1) may be written in terms of the radial and vertical cylindrical coordinates, ρ and z, as

$$\frac{\partial^2\Phi}{\partial\rho^2} + \frac{1}{\rho}\frac{\partial\Phi}{\partial\rho} + \frac{\partial^2\Phi}{\partial z^2} = 0 \tag{2}$$

A unique solution of (2) may be obtained by employing the method of separation of variables and imposing boundary conditions on the potential function consistent with the charge requirements on the conducting surfaces. This separates (2) into the following set of equations,

$$\Phi(\rho,z) = R(\rho)Z(z), \tag{3}$$

$$\frac{d^2R}{\partial\rho^2} + \frac{1}{\rho}\frac{dR}{d\rho} + k^2R = 0, \tag{4}$$

$$\frac{d^2Z}{dz^2} - k^2Z = 0, \tag{5}$$

where the parameter k is determined from the boundary requirements on Φ [2].

For this problem, the following boundary conditions are imposed on the potential function: The electric potential must vanish over the surface of the cylinder, maintain the constant value $\frac{1}{2}V$ over the top plate, maintain the constant value $-\frac{1}{2}V$ over the bottom plate, and approach a uniform field

potential in the z-direction as ρ approaches infinite. A single, analytical expression satisfying all boundary conditions could not be obtained from the differential equations (4) and (5) because of the insufficient number of boundary parameters. Hence, a solution for these equations within each of three limited regions between the plates was obtained, and the solutions within adjoining regions were matched at a common boundary. In this way, an expression for each potential function is determined in terms of the other potential functions, and a solution for each may then be obtained by iteration. The three regions delineated in Figure 3 were found convenient for satisfying the required boundary conditions. Because of symmetry about the cylinder axis, the solution regions are indicated for one half of the (ρ,z)-plane only. Solutions within the three areas are labeled $\Phi_{\hat{o}}$, $\Phi_{\hat{1}}$, $\Phi_{\hat{2}}$. Potential function $\Phi_{\hat{o}}$ was chosen to match the boundary conditions necessary for the region $\rho > a$ for $0 \leq z \leq d$; $\Phi_{\hat{1}}$ is valid within the region $0 \leq z \leq z_{\hat{1}}$ for $\rho \geq 0$; while $\Phi_{\hat{2}}$ is defined for the region $z_{\hat{2}} < z < d$ for $\rho \geq 0$. The solution $\Phi_{\hat{o}}$ overlaps the potential functions $\Phi_{\hat{1}}$ and $\Phi_{\hat{2}}$ in areas near the bottom and top plates, respectively. The total field is thus given by the solution for $\Phi_{\hat{o}}$ beyond $\rho = 0$ and by $\Phi_{\hat{1}}$ and $\Phi_{\hat{2}}$ for $0 \leq \rho \leq a$ near the bottom and top plates, respectively.

Since the solution $\Phi_{\hat{o}}$ must approach a uniform potential distribution at large ρ, one expects

$$\Phi_{\hat{o}} \rightarrow z \cdot C_{\hat{1}} + C_{\hat{2}}, \quad \text{as } \rho \rightarrow \infty. \tag{6}$$

Corresponding boundary conditions on the two plates require that

$$0 \cdot C_{\hat{1}} + C_{\hat{2}} = -\tfrac{1}{2}V \tag{7a}$$

$$d \cdot C_{\hat{1}} + C_{\hat{2}} = \tfrac{1}{2}V \tag{7b}$$

Thus, $C_{\hat{1}} = V/d$ and $C_{\hat{2}} = -\frac{1}{2}V$, so that

$$\lim_{\rho\to\infty} \Phi_{\hat{0}}(\rho,z) = V(z/d - \tfrac{1}{2}), \tag{8}$$

which represents the k = 0 solution of (5). Solutions for nonzero values of k must be added to (8) and must be chosen to satisfy the remaining boundary conditions on $\Phi_{\hat{0}}$; that is,

$$\Phi_{\hat{0}}(a,z) = 0, \text{ for } z_{\hat{1}} \le z \le z_{\hat{2}}, \tag{9a}$$

$$\Phi_{\hat{0}}(\rho,0) = -\tfrac{1}{2}V, \text{ for } \rho > a, \tag{9b}$$

$$\Phi_{\hat{0}}(\rho,d) = \tfrac{1}{2}V, \text{ for } \rho > a. \tag{9c}$$

These requirements impose the following conditions on the functions Z(z) and R(ρ) for nonzero k:

$$Z(0) = Z(d) = 0, \tag{10a}$$

$$R(\rho) \to 0, \text{ as } \rho \to \infty. \tag{10b}$$

This suggests that solutions of (5) are of the form sin(kz), while solutions of (4) are modified Bessel functions of the second kind $K_{\hat{0}}(k\rho)$, with

$$k = k_{\hat{n}} = n\pi/d, \quad \text{for } n = 1, 2, 3, \cdots. \tag{11}$$

A complete solution for the region ρ > a can thus be expressed as

$$\Phi_{\hat{0}}(\rho,z) = -V(d - 2z)/(2d) + \sum_{n=1}^{\infty} A_{\hat{n}} \sin(k_{\hat{n}}z)\, K_{\hat{0}}(k_{\hat{n}}\rho), \tag{12}$$

which is a Bessel-Fourier series expansion for the potential $\Phi_{\hat{0}}$. By matching this solution with those for the remaining two regions across the boundary $\rho = a$, the constants $A_{\hat{n}}$ may be evaluated as functions of n and the problem parameters V, a, d, $z_{\hat{1}}$, $z_{\hat{2}}$. The first step in accomplishing this evaluation takes advantage of the orthogonality of the trigonometric functions and the uniform convergence of the Fourier series by multiplying both sides of (12) by $\sin(k_{\hat{m}}z)$ and integrating from z = 0 to z = d (at $\rho = a$), with the result that

$$\int_0^d \left[\Phi_{\hat{0}}(a,z) + V(\tfrac{1}{2} - z/d)\right]\sin(k_{\hat{n}}z)dz = \tfrac{1}{2}dA_{\hat{n}}K_0(k_{\hat{n}}a). \tag{13}$$

But, since Φ_0 overlaps with Φ_1 and Φ_2, and since the cylinder is unchanged, we have

$$\Phi_{\hat{0}}(a,z) = \begin{cases} \Phi_{\hat{1}}(a,z) & \text{for } 0 < z < z_{\hat{1}} \\ 0 & \text{for } z_{\hat{1}} < z < z_{\hat{2}} \\ \Phi_{\hat{2}}(a,z) & \text{for } z_{\hat{2}} < z < d, \end{cases} \tag{14}$$

so that we may write

$$\tfrac{1}{2}dK_{\hat{0}}(k_{\hat{n}}a)A_{\hat{n}} = B_{\hat{n}} + C_{\hat{n}}, \tag{15}$$

with

$$B_{\hat{n}} = \int_0^{z_{\hat{1}}} \left[\Phi_{\hat{1}}(a,z) + V(\tfrac{1}{2} - z/d)\right]\sin(k_{\hat{n}}z)dz \tag{16}$$

$$+ \int_{z_{\hat{2}}}^d \left[\Phi_{\hat{2}}(a,z) + V(\tfrac{1}{2} - z/d)\right]\sin(k_{\hat{n}}z)dz \tag{16}$$

and

$$C_{\hat{n}} = -V/\{dk_{\hat{n}}^2\}\left[\sin(k_{\hat{n}}z_{\hat{2}}) - \sin(k_{\hat{n}}z_{\hat{1}}) - k_{\hat{n}}(z_{\hat{2}} + \tfrac{1}{2}d)\cos(k_{\hat{n}}z_{\hat{2}})\right. \quad (17)$$

$$\left. + k_{\hat{n}}(z_{\hat{1}} + \tfrac{1}{2}d)\cos(k_{\hat{n}}z_{\hat{1}})\right].$$

This completes the analytical development for the potential function $\Phi_{\hat{0}}$. Once the values for the functions $\Phi_{\hat{1}}(a,z)$ and $\Phi_{\hat{2}}(a,z)$ are determined, A_n may be evaluated from (15) and $\Phi_{\hat{0}}(\rho,z)$ is completely specified by the series expansion (12).

A uniform field distribution is also required for both $\Phi_{\hat{1}}$ and $\Phi_{\hat{2}}$ at large radii, and (8) is the k = 0 solution for each of these potential functions. Boundary conditions to be satisfied by these potential functions for nonzero k values are

$$\Phi_{\hat{1}}(\rho,0) = -\tfrac{1}{2}V, \quad (18a)$$

$$\Phi_{\hat{2}}(\rho,d) = \tfrac{1}{2}V, \quad (18b)$$

$$\Phi_{\hat{1}}(\rho,z_1) = \Phi_{\hat{2}}(\rho,z_{\hat{2}}) = 0, \quad \text{for } 0 < \rho < a. \quad (18c)$$

These conditions, along with (8), require that

$$Z_1(0) = Z_2(d) = 0, \quad (19a)$$

$$R_{\hat{1}}(\rho) = R_{\hat{2}}(\rho) \to 0, \text{ as } \rho \to \infty. \quad (19b)$$

Since Z_1 and Z_2 do not vanish on the surface of the cylinder, exponential functions of kz can be assumed. The requirements of (19a) then lead to:

$$Z_{\hat{1}}(z) = \sinh(kz), \tag{20a}$$

$$Z_{\hat{2}}(z) = \exp(kz) - \exp\left[k(2d - z)\right]. \tag{20b}$$

Corresponding solutions of (4) that satisfy (19b) are Bessel functions of the first kind of order zero:

$$R_{\hat{1}}(\rho) = R_{\hat{2}}(\rho) = J_{\hat{0}}(\rho k). \tag{21}$$

Solutions of Laplace's equation for $\Phi_{\hat{1}}$ and $\Phi_{\hat{2}}$ must then be expressed in terms of integrals of the functions (20) and (21), as

$$\Phi_{\hat{1}}(\rho,z) = -V(\tfrac{1}{2} - z/d) + \int_0^\infty F_{\hat{1}}(k')\sinh(k'z)J_{\hat{0}}(k\rho)dk', \tag{22}$$

$$\Phi_{\hat{2}}(\rho,z) = -V(\tfrac{1}{2} - z/d) + \int_0^\infty F_{\hat{2}}(k')\{\exp(k'z) - \exp\left[k'(2d - z)\right]\}$$

$$\times J_{\hat{0}}(k'\rho)dk'. \tag{23}$$

Evaluation of $F_{\hat{1}}(k)$ and $F_{\hat{2}}(k)$ is accomplished by applying the remaining boundary conditions and utilizing the orthogonality of the Bessel functions, where the integral of $\rho J_{\hat{0}}(k\rho)J_{\hat{0}}(k'\rho)$ with respect to ρ is nonzero and equal to $1/k$ only when $k' = k$. Hence, both sides of (23) may be multiplied by $\rho J_{\hat{0}}(k\rho)$ and integrated from $\rho = 0$ to $\rho = \infty$ (at $z = z_{\hat{2}}$), with the result that

$$\int_0^\infty \rho J_{\hat{0}}(k\rho)\left[\Phi_{\hat{2}}(\rho,z_{\hat{2}}) + V(\tfrac{1}{2} - z_{\hat{2}}/d)\right]d\rho$$

$$= F_2(k)\{\exp(kz_{\hat{2}}) - \exp\left[k(2d - z_{\hat{2}})\right]\}/k. \tag{24}$$

Boundary conditions on $\Phi_{\hat{2}}$ allow the integral on the left of (24) to be written as

$$\int_0^\infty \rho J_{\hat{0}}(k\rho)\left[\Phi_{\hat{2}}(\rho,z_{\hat{2}}) + V(\tfrac{1}{2} - z_{\hat{2}}/d)\right] d\rho \tag{25}$$

$$= V(\tfrac{1}{2} - z_{\hat{2}}/d) \int_0^a \rho J_{\hat{0}}(k\rho)d\rho$$

$$+ \int_a^\infty \rho J_{\hat{0}}(k\rho)\left[\Phi_{\hat{0}}(\rho,z_{\hat{2}}) + V(\tfrac{1}{2} - z_{\hat{2}}/d)\right] d\rho.$$

The first integral on the right of (25) may be expressed as a Bessell function of order one,

$$\int_0^a \rho J_{\hat{0}}(k\rho)d\rho = aJ_{\hat{1}}(ka)/k, \tag{26}$$

while the second integral on the right of (25) may be rewritten using (12) as

$$\int_0^\infty \rho J_{\hat{0}}(k\rho)\left[\Phi_{\hat{0}}(\rho,z_{\hat{2}}) + V(\tfrac{1}{2} - z_{\hat{2}}/d)\right] d\rho \tag{27}$$

$$= \sum_{n=1}^\infty A_{\hat{n}} \sin(k_{\hat{n}} z_{\hat{2}}) \int_a^\infty \rho K_{\hat{0}}(k_{\hat{n}}\rho) J_{\hat{0}}(k_{\hat{n}}\rho)d\rho.$$

An evaluation of the integral appearing in (27) may be obtained from the defining equations for K_0 and J_0 [3, P. 358], which are

$$\rho^2 \frac{d^2}{d\rho^2} K_{\hat{0}}(k_{\hat{n}}\rho) + \rho \frac{d}{d\rho} K_{\hat{0}}(k_{\hat{n}}\rho) - k_{\hat{n}}^2\rho^2 = 0 \tag{28}$$

and

$$\rho^2 \frac{d^2}{d\rho^2} J_{\hat{0}}(k\rho) + \rho \frac{d}{d\rho} J_{\hat{0}}(k\rho) + k^2\rho^2 = 0. \tag{29}$$

If (28) is multipled by $J_{\hat{o}}(k\rho)/\rho$, (29) is multiplied by $K_{\hat{o}}(k_{\hat{n}}\rho)/\rho$, and the resulting equations are subtracted and integrated over the interval $a \leq \rho < \infty$, we have

$$(k^2 + k_{\hat{n}}^2) \int_a^\infty \rho J_{\hat{o}}(k\rho)K_{\hat{o}}(k_{\hat{n}}\rho)d\rho \tag{30}$$

$$= -\{\rho\left[K_{\hat{o}}(\rho k_{\hat{n}}) \frac{d}{d\rho} J_{\hat{o}}(k\rho) - J_{\hat{o}}(k\rho) \frac{d}{d\rho} K_{\hat{o}}(\rho k_{\hat{n}})\right]\}_a^\infty .$$

However,

$$\frac{d}{d\rho} J_{\hat{o}}(k\rho) = -kJ_{\hat{1}}(k\rho), \tag{31a}$$

$$\frac{d}{d\rho} K_{\hat{o}}(k_n\rho) = -k_{\hat{n}}K_{\hat{1}}(k_{\hat{n}}\rho), \tag{31b}$$

so that

$$\int_a^\infty \rho J_{\hat{o}}(k\rho)K_{\hat{o}}(k_{\hat{n}}\rho)d\rho = \left[k_{\hat{n}}J_{\hat{o}}(ka)K_{\hat{1}}(k_{\hat{n}}a)-kK_{\hat{o}}(k_{\hat{n}}a)J_{\hat{1}}(ka)\right]$$

$$a/(k^2 + k_{\hat{n}}^2), \tag{32}$$

and the final expression for $F_{\hat{2}}(k)$ is

$$F_{\hat{2}}(k) = \{Va(d - 2z_{\hat{2}})J_{\hat{1}}(ka)/(2dk) \tag{33}$$

$$+ \sum_{n=1}^{\infty} A_{\hat{n}}\sin(k_{\hat{n}}z_{\hat{2}}) \left[k_{\hat{n}}J_{\hat{o}}(ka)K_{\hat{1}}(k_{\hat{n}}a)\right.$$

$$\left. - kK_{\hat{o}}(k_{\hat{n}}a)J_{\hat{1}}(ka)\right] a/(k^2 + k_{\hat{n}}^2)\}k/Z_{\hat{2}}(z_{\hat{2}}),$$

where $Z_{\hat{2}}(z_{\hat{2}})$ is defined in (20b).

The evaluation of $F_{\hat{1}}(k)$ proceeds similarly, with the result that

$$F_{\hat{1}}(k) = \{Va(d - 2z_{\hat{1}})J_{\hat{1}}(ka)/(2dK) + \sum_{n=1}^{\infty} A_{\hat{n}}\sin(k_{\hat{n}}z_{\hat{1}})\left[k_{\hat{n}}J_{\hat{0}}(ka)K_{\hat{1}}(ka)\right.$$

$$\left. - kK_{\hat{0}}(k_{\hat{n}}a)J_{\hat{1}}(ka)\right] a/(k^2 + k_{\hat{n}}^2)\}k/\sinh(kz_{\hat{1}}). \qquad (34)$$

Evaluation of the distribution functions $\Phi_{\hat{0}}$, $\Phi_{\hat{1}}$, $\Phi_{\hat{2}}$ may now be obtained through a numerical evaluation of the coupled equations (15), (33) and (34).

Analytical expressions for the electric field intensity may be obtained in an area of interest by taking the appropriate derivative of one of the three potential functions. As an illustration, the electric field vector is perpendicular to any conducting surface; therefore, along the side of the cylinder, the electric field intensity is

$$E = \left.\frac{\partial\Phi_{\hat{0}}}{\partial\rho}\right|_{\rho = a} \qquad (35)$$

$$= \sum_{n=1}^{\infty} A_{\hat{n}}k_{\hat{n}}\sin(k_{\hat{n}}z)K_{\hat{1}}(k_{\hat{n}}a).$$

Similarly, over the top of the cylinder, we have

$$E = -\left.\frac{\partial\Phi_{\hat{2}}}{\partial z}\right|_{z = z_2} \qquad (36)$$

$$= V/d - \int_0^{\infty} kF_{\hat{2}}(k)J_{\hat{0}}(k\rho)\{\exp(kz_{\hat{2}}) + \exp\left[k(2d - z_{\hat{2}})\right]\}dk.$$

Field values may be obtained for electric field expressions such as (35) or (36) using the same numerical techniques to be discussed in the next section.

3. NUMERICAL EVALUATION

In order to produce coupled equations in terms of the potential functions directly, relations (33) and (34) are substituted into (23) and (22), respectively, yielding

$$\Phi_{\hat{1}}(\rho,z) = Va(\tfrac{1}{2} - z_{\hat{1}}/d) \int_0^\infty J_{\hat{0}}(k\rho)J_{\hat{1}}(ka)Z_{\hat{1}}(kz)/\left[Z_{\hat{1}}(kz_{\hat{1}})\right]dk \qquad (37)$$

$$+ \sum_{n=1}^{\infty} aA_{\hat{n}}\sin(k_{\hat{n}}z_{\hat{1}})\{k_{\hat{n}}K_{\hat{1}}(k_{\hat{n}}a) \int_0^\infty J_{\hat{0}}(k\rho)J_{\hat{0}}(ka)$$

$$\times kZ_{\hat{1}}(kz)/\left[(k^2 + k_{\hat{n}}^2)Z_{\hat{1}}(kz_{\hat{1}})\right]dk$$

$$- K_{\hat{0}}(k_{\hat{n}}a) \int_0^\infty J_{\hat{0}}(k\rho)J_{\hat{1}}(ka)k^2Z_{\hat{1}}(kz)/\left[(k^2 + k_{\hat{n}}^2)Z_{\hat{1}}(kz_{\hat{1}})\right]dk\}$$

$$- V(\tfrac{1}{2} - z/d),$$

$$\Phi_{\hat{2}}(\rho,z) = Va(\tfrac{1}{2} - z_{\hat{2}}/d) \int_0^\infty J_{\hat{0}}(k\rho)J_{\hat{1}}(ka)Z_{\hat{2}}(kz)/\left[Z_{\hat{2}}(kz_{\hat{2}})\right]dk \qquad (38)$$

$$+ \sum_{n=1}^{\infty} aA_{\hat{n}}\sin(k_{\hat{n}}z_{\hat{2}})\{k_{\hat{n}}K_{\hat{1}}(k_{\hat{n}}a) \int_0^\infty J_{\hat{0}}(k\rho)J_{\hat{0}}(ka)$$

$$\times kZ_{\hat{2}}(kz)/\left[(k^2 + k_{\hat{n}}^2)Z_{\hat{2}}(kz_{\hat{2}})\right]dk$$

$$- K_{\hat{0}}(k_{\hat{n}}a) \int_0^\infty J_{\hat{0}}(k\rho)J_{\hat{1}}(ka)k^2Z_{\hat{2}}(kz)/\left[(k^2 + k_{\hat{n}}^2)Z_{\hat{2}}(kz_{\hat{2}})\right]dk\}$$

$$- V(\tfrac{1}{2} - z/d),$$

where the functions $Z_{\hat{1}}$ and $Z_{\hat{2}}$ are as defined in equations (20). With all potential functions now expressed in terms of $A_{\hat{n}}$, a straightforward procedure is to assume functional forms for $\Phi_{\hat{1}}$ and $\Phi_{\hat{2}}$ along the surface $\rho = a$, obtain $A_{\hat{n}}$ from (15) and evaluate $\Phi_{\hat{1}}$ and $\Phi_{\hat{2}}$ along $\rho = a$ from (37) and (38). These calculated values may then be compared to the starting functions at selected points. If agreement is not close enough, the calculated values may then be used to recalculate $A_{\hat{n}}$, $\Phi_{\hat{1}}$, and $\Phi_{\hat{2}}$. This process can be repeated until the required convergence is reached.

Several starting approximations were tried for $\Phi_{\hat{1}}$ and $\Phi_{\hat{2}}$ along $\rho = a$. It was found that the particular functional form for the initial values of the potentials had little effect on convergence. Figure 4 is a plot of the calculated electric field potential after four iterations. This run used the following linear, initial approximations to $\Phi_{\hat{1}}$ and $\Phi_{\hat{2}}$ along the surface $\rho = a$,

$$\Phi_{\hat{1}}(a,z) = \tfrac{1}{2}V(z - z_{\hat{1}})/z_{\hat{1}}, \tag{39a}$$

$$\Phi_{\hat{2}}(a,z) = \tfrac{1}{2}V(z - z_{\hat{2}})/(d - z_{\hat{2}}). \tag{39b}$$

All series were calculated with convergence criteria of 0.001 or 500 terms. Integrals over the Bessel functions were evaluated using Simpson's rule and dividing the interval between zeros of the integrand into ten equal subdivisions. Calculations were carried through 500 oscillations of the integrand. The formulas used for calculating these zeros are[4].

$$x_{\hat{n}} \simeq b + 1/(8b), \quad n = 1,2,3,\cdots, \tag{40}$$

$$b = \pi(n - \tfrac{1}{4})$$

for $J_o(x)$, and

$$x_{\hat{n}} \simeq b - 3/(8b), \quad n = 1,2,3,\cdots, \tag{41}$$

$$b = \pi(n + \tfrac{1}{4})$$

for $J_{\hat{1}}(x)$.

Polynomial approximations [3,369-370, 378-379] were used to evaluate all Bessel functions to an accuracy of about 10^{-7}. In addition, the following approximations were used in the calculations to evaluate ratios of exponential functions:

$$\frac{Z_{\hat{2}}(kz)}{Z_{\hat{2}}(kz_{\hat{2}})} \simeq \exp\left[-k(z - z_{\hat{2}})\right]\left\{1 - \exp\left[-2k(d - z)\right]\right\} \tag{42}$$

$$\text{for } 2d(d - z_{\hat{2}}) > 100,$$

$$\simeq \exp\left[-k(z - z_{\hat{2}})\right] \text{ for } 2k(d - z) > 100,$$

$$\simeq 0 \text{ for } k(z - z_{\hat{2}}) > 100.$$

The parameter set used for the calculations in Figure 4 are $V = 1$, $a = 0.02$, $d = 1$, $z_{\hat{1}} = 0.06$, $z_{\hat{2}} = 0.36$.

4. CONCLUSION

Evaluation of the electric field surrounding a conducting cylinder between charged plates may be accomplished directly from Laplace's equation. This evaluation is valid for either a static field or a transmission line propagating the TEM mode. However, the boundary conditions for this problem requires an indirect approach. A general approach that may be taken in this class of problems is to solve Laplace's equation by separation of variables in overlapping regions of the problem space. All parameters may then be resolved by applying boundary conditions and matching solutions along common surfaces.

The result for this particular application is a set of three coupled, nonlinear equations for the electric potential function, which are solved numerically by iteration. Figure 4 maps the calculated potential for one geometry. Boundary conditions have been satisfied exactly over all conducting surfaces, and the field approaches a uniform potential at approximately twenty radii from the cylinder axis. This illustration depicts the numerical solution after four iterations, using linear starting approximations for the potential along $\rho = a$.

The numerical solution to the coupled equations derived from Laplace's equation, for this example, were carried through using various starting functional forms for the potential (polynomial and exponential) and a varying number of iterations. In all cases, convergence was observed to be fairly close even after just one iteration. Boundary conditions, after one iteration, were exactly satisfied over all conducting surfaces. The

field was found to be nearly uniform at approximately thirty radii from the cylinder axis. Subsequent iterations produced fairly rapid convergence. The major contribution to error in this example is in the evaluation of the integrals appearing in the series solution for the potential. These infinite integrals converge slowly in certain regions due to the presence of Bessel functions of the first kind.

This paper has presented one specific solution of a general technique that may be used to obtain the electrostatic field surrounding interacting conductors. Computer solutions provided accurate field values for this specific case even after only one iteration. No attempt has been made to compare this approach to other techniques that may be used to approximate solutions of Laplace's equation.

REFERENCES

[1] M. Abramowitz and I. A. Stegun. Handbook of Mathematical Functions. Dover Publ., New York, 1965.

[2] D. D. Hearn, M. Summers and E. J. Driesse. To be published.

[3] P. M. Morse and H. Feshbach. Methods of Theoretical Physics. McGraw-Hill Book Co., New York, 1953, Vol. II, Chapt. 10, 1259-1262.

[4] G. N. Watson. A Treatise on the Theory of Bessel Functions. Cambridge Univ. Press, 2nd Ed., 1962, 505.

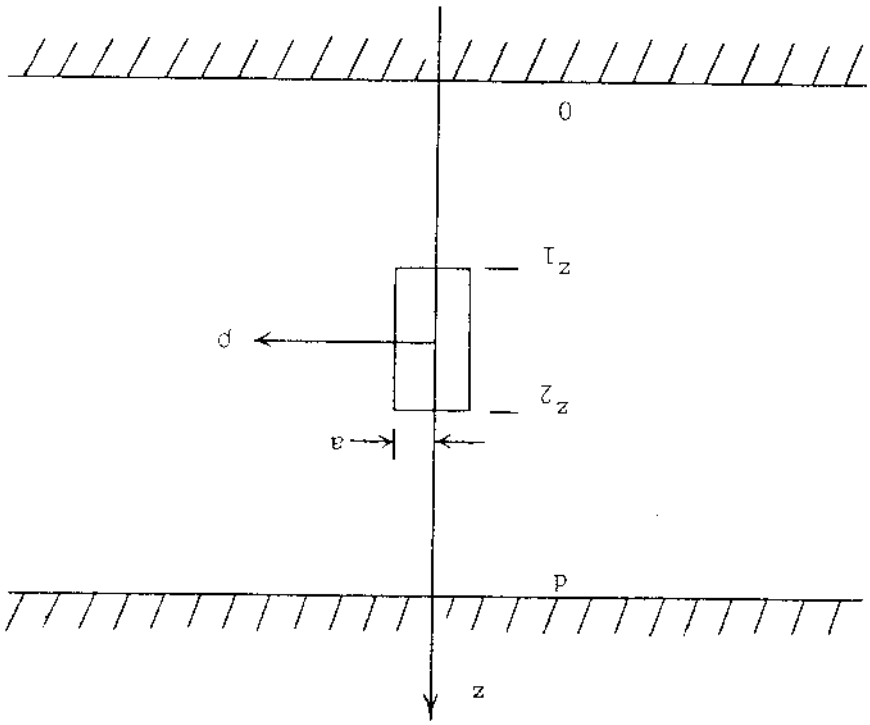

Figure 2

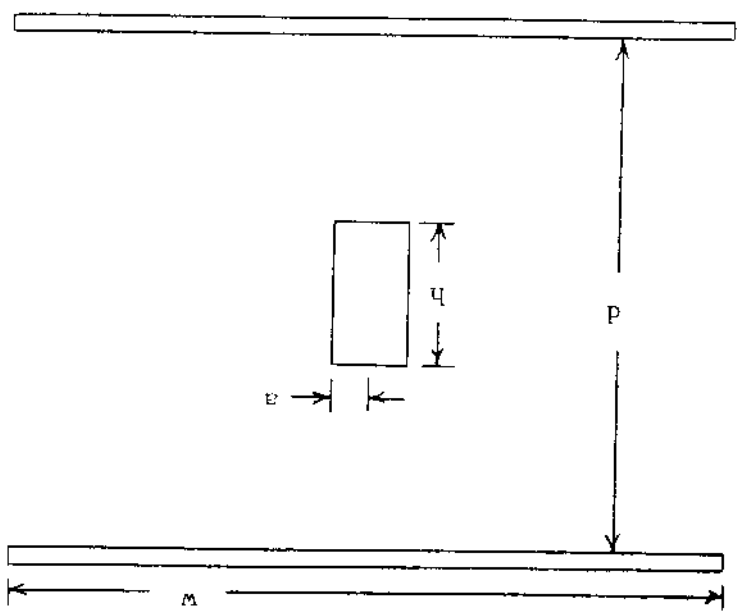

Figure 1

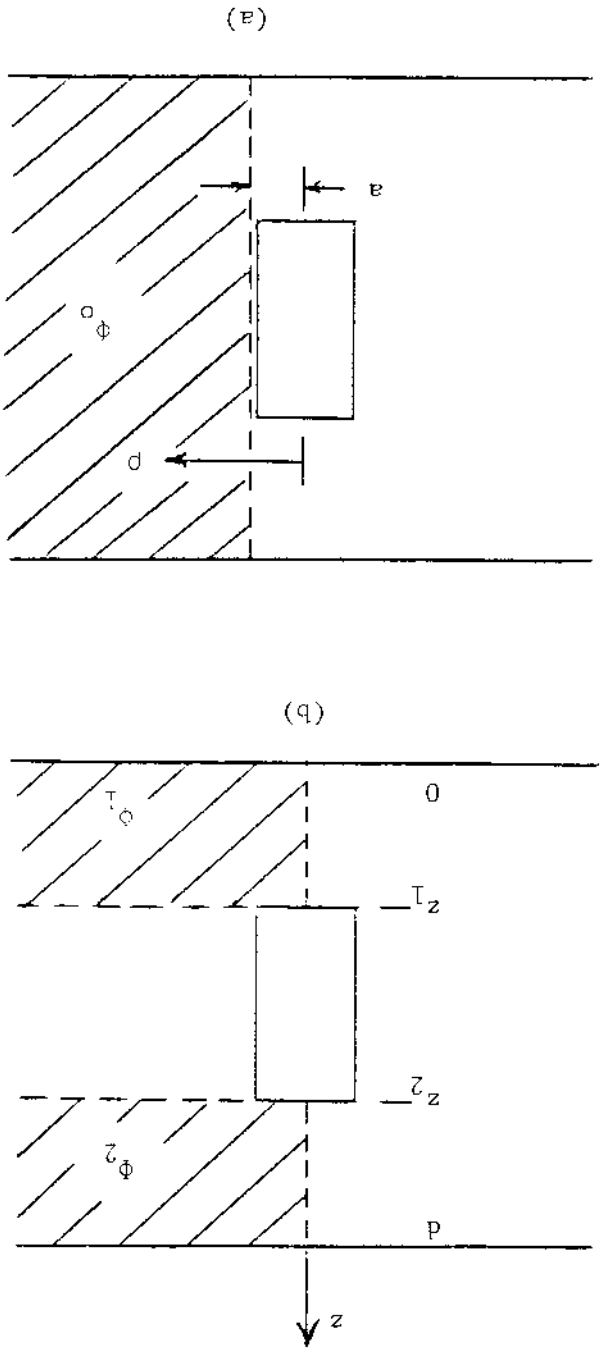

Figure 3

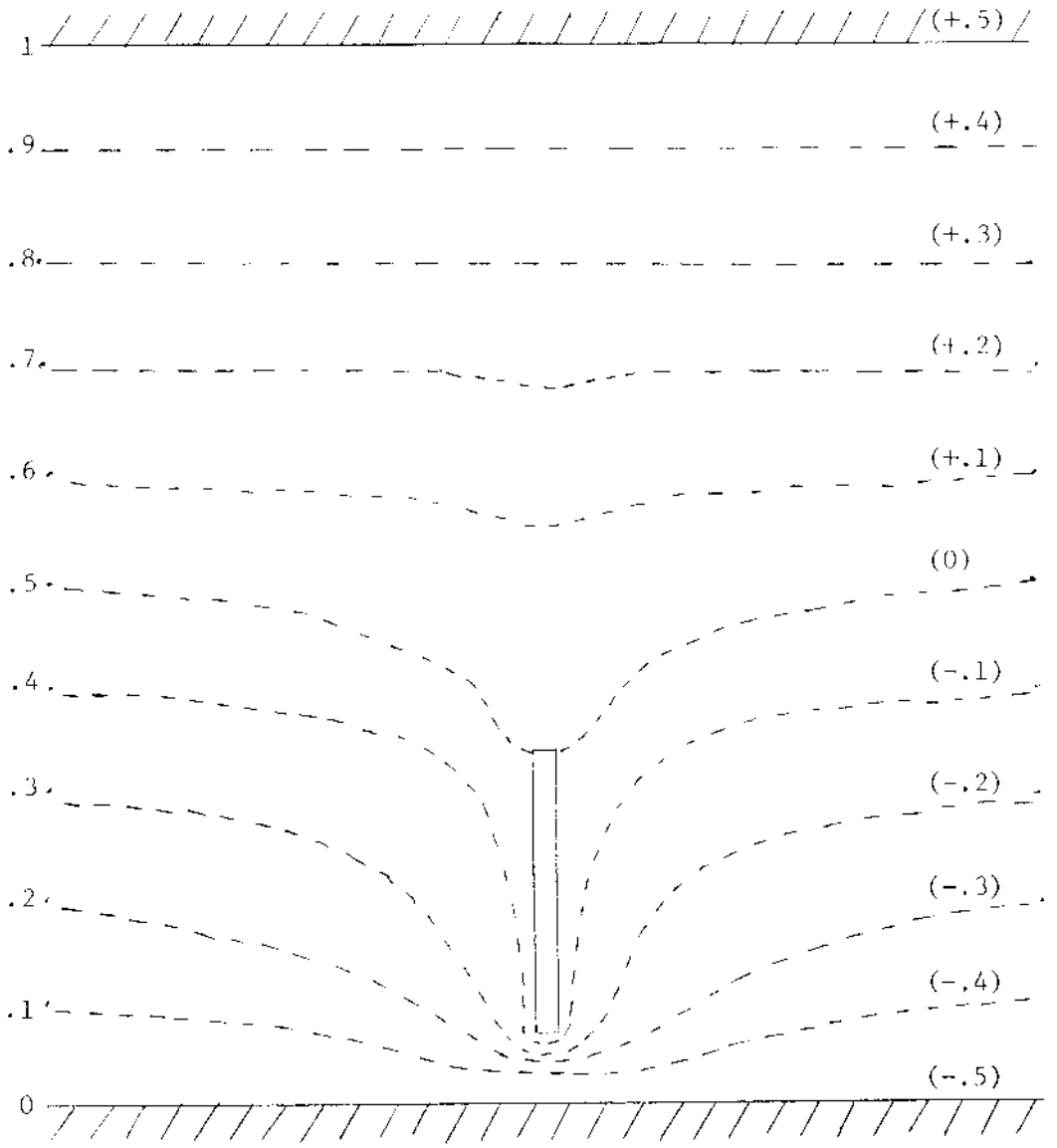

Figure 4